Kinetic studies on the hydrothermal crystallization of Co-doped nanostructured TiO_2 anatase with ferromagnetic properties

R. R PITICESCU[a], S. N. VALSAN[a] M. PETRICEANU[a], V. BADILITA[a], I. A. TUDOR[a*], D. TALOI[a], B. VASILE[b], O. RAITA[c]
[a]*National R&D Institute for Non-Ferrous and Rare Metals, 102 Biruintei blvd., Pantelimon, Ilfov, 077145 Romania*
[b]*University Politehnica Bucharest, Faculty of Applied Chemistry and Materials Science, 313 Splaiul Independentei, Bucharest, Romania*
[c]*National R&D Institute of Isotopes and Molecular Technologies, 65-103 Donath Str., 400293 Cluj-Napoca 5, România*

Nanopowders based on Co-doped TiO_2 anatase (with Co content in the range 0-5 at %) with rod-like structure and homogeneous distribution of the doping agent were obtained by hydrothermal synthesis in the temperature range 200-275^{0}C in the presence of KOH as mineralizing agent. The kinetic triplet of crystallization (activation energy, reaction orders and pre-exponential factors) were calculated from DSC measurements using Avrami-Erofeev equation. For pure TiO_2 the best fitting reaction order was found n=1 while for 2.5 and 5 at% Co-doped TiO_2 the reaction order is n=2/3. The evolution the activation energy with increasing Co content may be attributed to the increasing of defects in the crystalline lattice, as suggested by EPR results. The EPR investigations show also different ferromagnetic behaviours with increasing Co concentration.

(Received November 6, 2014; accepted May 7, 2015)

Keywords: Hydrothermal synthesis, activation energy, Co-doped anatase, nanosize particles, EPR

1. Introduction

Diluted magnetic semiconductor oxides (DMO) based on Co-doped TiO_2 (CTO) materials have received a high interest due to their ferromagnetic properties with high potential in spintronic and magnetic device applications [1-3]. The origin of ferromagnetism in CTO materials is strongly dependant on doping concentration and distribution and the presence of lattice defects such as oxygen vacancies. Consequently obtaining of nanopowders allowing stabilization of non-equilibrium phases is expected to strongly influence the ferromagnetic and spin dynamics properties of these materials [4, 5].

Different chemical, physical or combined methods have been reported for the synthesis of pure and doped TiO_2 nanomaterials with different structures and morphologies [6]. Hydrothermal synthesis is one of the methods enabling to produce nanocrystalline powders in one step process at low temperatures from a wide range of soluble or amorphous precursors [7]. However prediction and selection of optimal pH range, temperature, duration and mineralizing agents controlling both powders morphology and Co distribution is a challenge [8, 9].

Titanium dioxide crystallizes in three different structures: rutile (generally the most stable one), anatase and brookite. Anatase is reported to have increased surface activity observed mainly in studies related to their enhanced photo-catalytic activity. Hwu et al. show that for small TiO_2 nanoparticules (< 50 nm), anatase seemed more stable and transformed to rutile at > 973 K and they found that the crystal structure of TiO_2 nanoparticules depended largely on the preparation method [10]. Banfield et al. prepared TiO2 nanoparticules with anatase and/or brookite structures, which transformed to rutile after reaching a certain particule size [11, 12]. Once rutile was formed, it grew much faster than anatase and became more stable than anatase for a critical particle size > 14 nm. Ranade et al. found that the rutile was energetically stable for specific surface area < 592 m^2/mol (7 m^2/g or < 200 nm), brookite was energetically stable from < 592 to 3174 m^2/mol (7 – 40 m^2/g or 200 - 40 nm) and anatase was energetically stable for greater surface areas or smaller sizes (< 40 nm) [13].

In the temperature range of 973 – 1073 K only anatase and rutile phase transformation were observed and both their particles sizes increased with the increase of temperature. With the decrease of initial particle size, the onset transition temperature was decreased. The value for the activation energies obtained were 299, 236, and 180 kJ/ mol for 23, 17 and 12 nm TiO_2 nanoparticles, respectively [14]. In [15] non-isothermal methods were used to evaluate the kinetic parameters for the crystallization of TiO_2 prepared by hydrolysis method from DSC data. Depending on the applied kinetic equations used (Kissinger, Ozawa and Kazeev-Yerofeev) activation energies of crystallization values of 160, 171 and 181kJ/mol were respectively obtained.

Mehranpour et al. synthesized titanium dioxide nanopowders by the diffusion controlled sol-gel (LaMer model) and characterized by DTA-TG, XRD and SEM. The prepared TiO_2 nanoparticles have uniform size and morphology, and the phase transformation kinetics of

obtained material was studied by interpretation of the X-ray diffraction patterns peaks on the base of Avrami equation [16]. Traces of ferric oxide have a strong catalytic effect on both nucleation and growth phases of the transformation of TiO_2 from anatase to rutile. A detailed study on the Fe2O3/TiO2 thermal behavior of mesoporous gels showing the crystallization of anatase is presented in [17]. This effect is greatly enhanced in atmospheres with low oxygen content. Using TG, DTA, XRD, BET and TEM the effects of aging on crystallite sizes agglomeration of TiO_2 gels was investigated. The activation energy values for crystallite growth in samples after aging treatment were greater than that found in un-aged sample [18]. In a later study, Zhang and Banfield studied by X-ray power diffraction and transmission electron microscopy (TEM) the kinetics of crystallization and crystal growth of nanocrystalline anatase in amorphous titania samples (2.5 – 3 nm) in the temperature range 300 - 400°C [19]. The chemical species evolved during pyrolysis studies of sol-gel derived TiO_2 powders for temperatures up to 350^0C before crystallization of anatase phase were revealed by Compostrini et al. [20, 21].

In the present paper, the kinetic of hydrothermal crystallization process of nanocrystalline TiO_2 anatase doped with 2.5 and 5 at % Co was investigated. The kinetic triplet (activation energy, pre-exponential factor and reaction order) for pure and Co-doped TiO2 anatase was calculated based on different linear iso-conversional analysis methods from DSC measurement. Finally, the influence of Co concentration on the intrinsic spin dynamic properties of nanocrystalline anatase powders has been studied by EPR method.

2. Experimental

2.1 Materials and Synthesis

High purity titanium (IV) chloride from Fluka Analytical, cobalt acetate $Co(CH_3COO)_2.2H_2O$, ammonia solution 25% and potassium hydroxide pellets from Chimopar S.A. were used in the synthesis without any further purification.

Firstly an aqueous solution with controlled concentration of Ti(IV) ions was obtained by dissolution of Ti(IV) chloride under stirring in distilled water in the presence of hydrogen peroxide (H_2O_2). Cobalt acetate was also dissolved in distilled water to get a solution with controlled Co (II) concentration. The two solutions were mixed in an appropriate volume ratio to obtain a mixed solution with 2.5 and 5 at % Co respectively. The pH of the solution was then adjusted to the desired experimental value by addition of ammonia and KOH solution and the resulting colloidal suspension was treated in a CORTEST Teflon autoclave in the temperature range 200^0C to 275^0C and times from 10 minutes to 120 minutes. The detailed procedure is described in [22]. The final precipitate was filtered, washed with water several times to eliminate soluble impurities and dried in an oven to constant weight.

2.2 Characterization methods

Chemical analysis of all initial solutions and final powders was accomplished by Atomic absorption spectrometry (AAS ZEEnit 700, Analytic Jena AG) and Indirect Plasma Coupled Spectrometry (ICP Spectroflame). Phase analysis was carried out at room temperature by XRD (Bruker D8 Advance) using CuK_α radiation with a wavelength λ=1.5406 Å and the help of DIFFRAC^{plus} BASIC (Bruker AXS) software and ICDD PDF-2 Release 2006 database. A small amount of powder was diluted into pure ethylic alcohol and left into an ultrasonic bath for approximately 15 minutes. After that, a small drop of the diluted solution was put onto a 400 mesh, holey carbon coated film Cu grid and left to dry for 30 minutes, prior to TEM investigation. The bright field and high resolution images were obtained using a Tecnai^{TM} G^2 F30 S-TWIN Transmission Electron Microscope (FEI, the Nederlands), equipped with a STEM/HAADF detector, EDX (Energy Dispersive X-ray analysis) and EFTEM-EELS spectrometer (Electron Energy Loss Spectroscopy).

Differential Scanning Calorimetry (DSC) measurements have been performed on a Netzsch DSC200 *F3 Maia* thermal analysis system, in the temperature range -40….600^{o}C. Data analysis was performed with the help of Proteus software. The first step was to determine the base (correction) line. The mass of aluminum crucibles was measured with 10^{-3} mg accuracy and subsequently introduced in the DSC furnace. The treatment was run in 50 ml/min Ar flow and in the temperature range - 40 … 600^{o}C. The equipment calibration was done with a sapphire standard sample, recorded using the previously measured base line and in the same treatment conditions – Ar atmosphere and temperature interval. The same base line was used to record the DSC curves of the doped TiO_2 samples.

Electron paramagnetic resonance (EPR) measurements of powder samples were carried out in the X-band at variable temperatures using a Bruker E-500 ELEXSYS spectrometer. The spectra processing was performed by Bruker Xepr software.

3. Results and discussions

3.1 Phase analysis

The XRD spectra of co-doped TiO_2 powders synthesized at different temperatures are presented in Fig. 1. It may be seen that all peaks indexed for both 2.5 and 5at% Co doping are corresponding to anatase structure (JCPDF 65-5714).

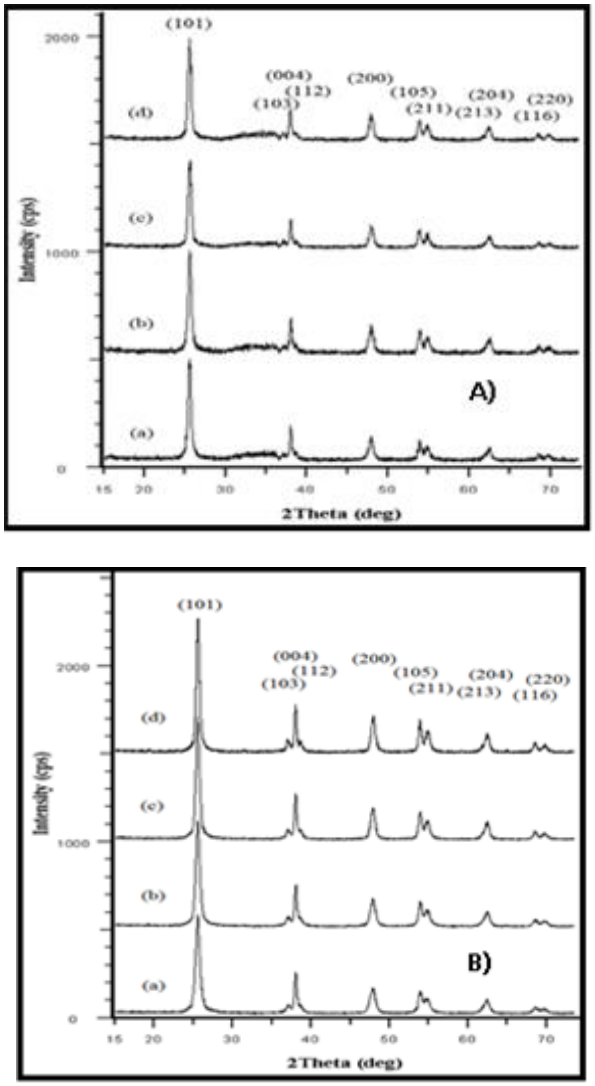

Fig.1. X-ray powder diffraction patterns for (A) 2.5Co-TiO_2 and (B) 5Co-TiO_2 powders doped with (a) 2.5 and (b) 5 at% Co hydrothermally synthesized at 200; 225; 250 and 275 ^0C

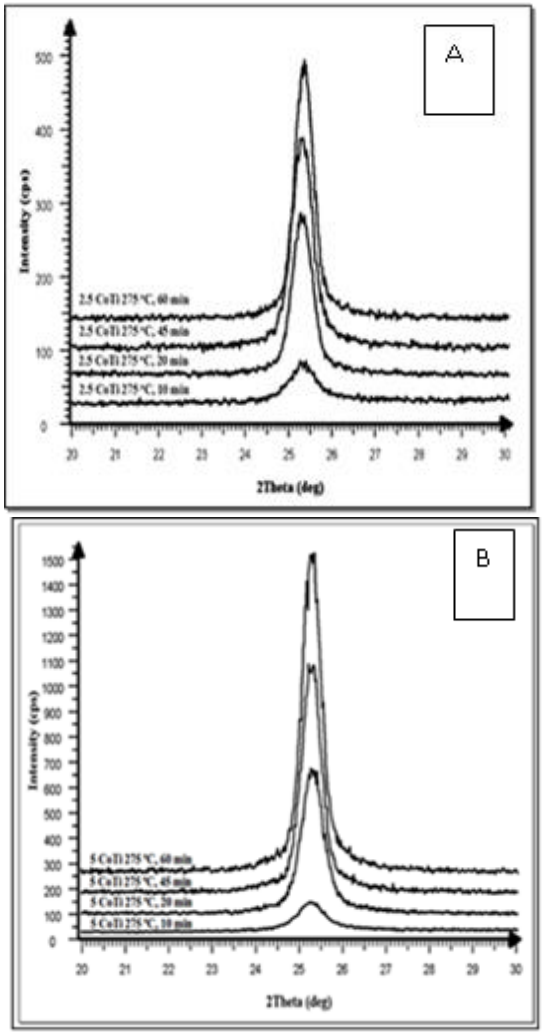

Fig. 2. X-ray powder diffraction patterns for TiO_2 powders doped with (a) 2.5 and (b) 5 at% Co hydrothermally synthesized at 275^0C for 10; 20; 45 and 60 min.

Fig. 2 presents the evolution of the major characteristic peak [101] from the XRD pattern of 2.5 and 5at% Co-doped anatase powders respectively, obtained at 275^{0}C for different hydrothermal treatment time. This peak was used to calculate the crystalline sizes of powders obtained at different synthesis parameters. The estimation was done from the broadening of [101] peak using Scherrer formula $D=0.9\ \lambda / \beta\cos\ /$, where D is the mean crystallite size, λ is the wavelength of the X-ray radiation, β is the width of the peak at half – maximum height and $/$ is the diffraction angle.

Table 1 presents the evolution of mean crystallite sizes vs. hydrothermal temperature and time. These results clearly show that all Co-doped TiO_2 powders are nanocrystalline. The average mean crystallite sizes of 2.5 at% Co-doped TiO_2 grows from11 nm to a maximum of 19 nm with increasing hydrothermal synthesis temperature from 200 to 275 ^{0}C and time in the range 10-120 min. For.5 at% Co-doped TiO_2 the average mean crystallite sizes grows from 9 to 17 nm in the same hydrothermal temperature and time range.

Table 1. Mean crystallite sizes of Co-doped TiO2 powders

Sample code	Temperature (ºC)	Time (s)	D (nm)	Sample code	Temperature (ºC)	Time (s)	D (nm)
2.5CoTi200t2	200	2700	11	5CoTi200t1	200	600	9
2.5CoTi200t3	200	3600	16	5CoTi200t3	200	2700	12
2.5CoTi200t4	200	7200	17	5CoTi200t4	200	3600	13
2.5CoTi225t2	225	2700	13	5CoTi200t6	200	7200	17
2.5CoTi225t3	225	3600	17	5CoTi225t3	225	2700	11
2.5CoTi225t4	225	7200	17	5CoTi225t4	225	3600	13
2.5CoTi250t1	250	600	13	5CoTi225t6	225	7200	16
2.5CoTi250t7	250	1200	14	5CoTi250t1	250	600	10
2.5CoTi250t8	250	1800	14	5CoTi250t3	250	2700	13
2.5CoTi250t3	250	2700	14	5CoTi250t4	250	3600	15
2.5CoTi250t4	250	3600	18	5CoTi250t6	250	7200	16
2.5CoTi250t6	250	7200	19	5CoTi275t1	275	600	11
2.5CoTi275t1	275	600	13	5CoTi275t3	275	2700	15
2.5CoTi275t3	275	2700	16	5CoTi275t4	275	3600	17
2.5CoTi275t4	275	3600	18	5CoTi275t6	275	7200	17
2.5CoTi275t6	275	7200	19				

3.2 TEM and HREM analysis

The morphology of the hydrothermally synthesized powders has been revealed by TEM studies. As an example, the TEM bright field image obtained on powders 2.5CoTi250t6 shown in fig. 3 reveals that the powder is composed from rod like shaped particles, with an average grain size of approximately 55.61 in length and 16.20 nm in width (Fig. 3.a). The nanopowders also have the tendency to form soft agglomerates (Fig.3b)

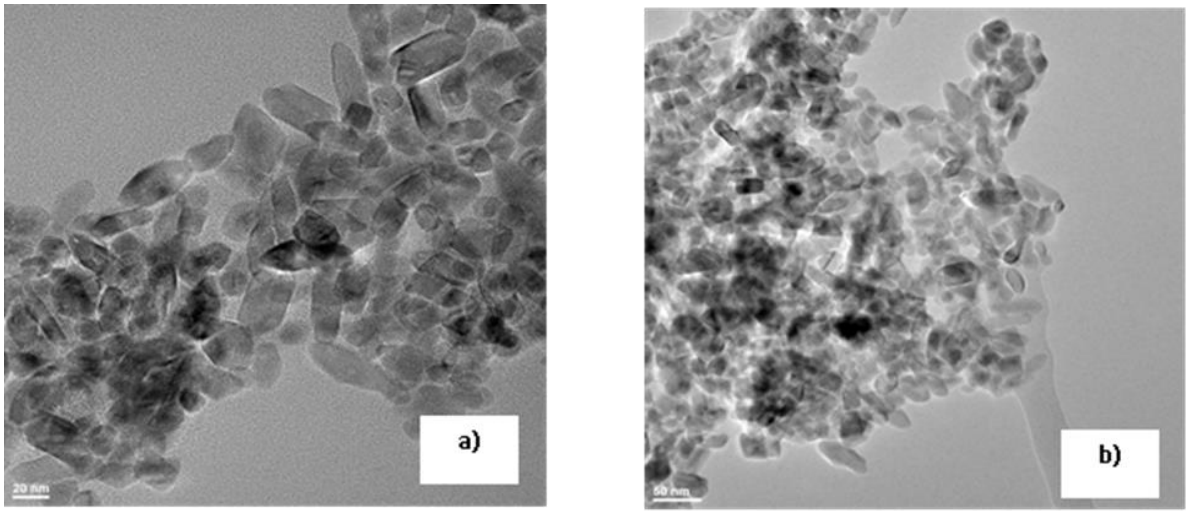

Fig 3. Bright field TEM image of 2.5 at% Co-doped TiO_2 sample hydrothermally synthesized 120 min. at 250 ^0C

The HRTEM image obtained on nanocrystalline sample is shown in Fig. 4 a. The image shows clear lattice fringes of polycrystalline nanopowder at d = 3.51 and 1.70 Å corresponding to the (1 0 1) and (1 0 5) crystallographic planes of TiO_2 anatase. Also the regular succession of the atomic planes indicates that all nanocrystalites are structurally uniform and crystalline with almost no amorphous phase present.

From the selected area diffraction pattern obtained on 2.5CoTi$O_2$250t6 nanopowders presented in Fig. 4b one can confirm that the only phase identified is the polycrystalline tetragonal phase of TiO_2 anatase.

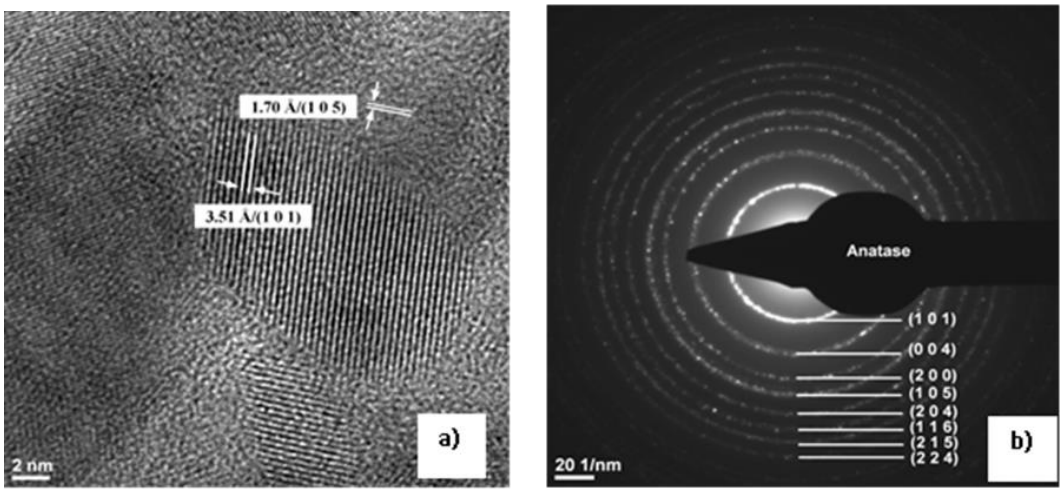

Fig 4. HR-TEM (a) and SAED (b) images of 2.5 at% Co-doped TiO_2 sample hydrothermally synthesized 120 min. at 250 ^0C

The TEM bright field image obtained on $5CoTiO_2250t6$ sample shown in fig. 5 reveals the formation of rod like particles, with an average grain size of approximately 79.12 nm in length and 15.65 in width.

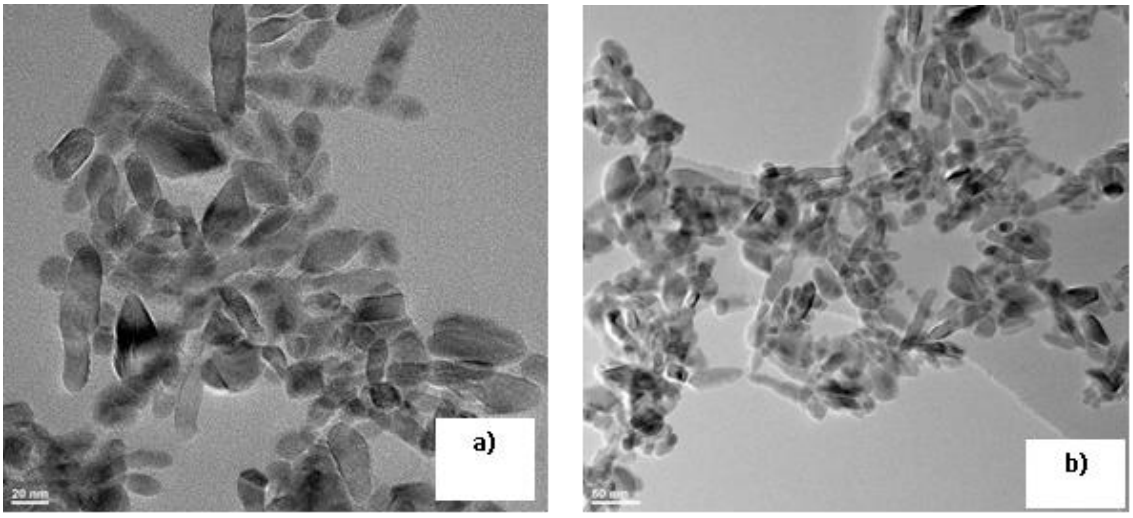

Fig 5. Bright field TEM image of 5 at% Co-doped TiO_2 sample hydrothermally synthesized 120 min. at 250 ^0C

The HRTEM image obtained on the sample is shown in Fig. 6 a. The image shows clear lattice fringes of polycrystalline nanopowder of d = 3.51 and 1.89 Å corresponding to the (1 0 1) and (2 0 0) crystallographic planes of TiO_2 anatase. Also the regular succession of the atomic planes indicates that the nanocrystalites are structurally uniform and crystalline with almost no amorphous phase present. It may therefore be stated that the only phase identified is the polycrystalline tetragonal phase of TiO_2 anatase for both 2.5 and 5 at % Co-doping.

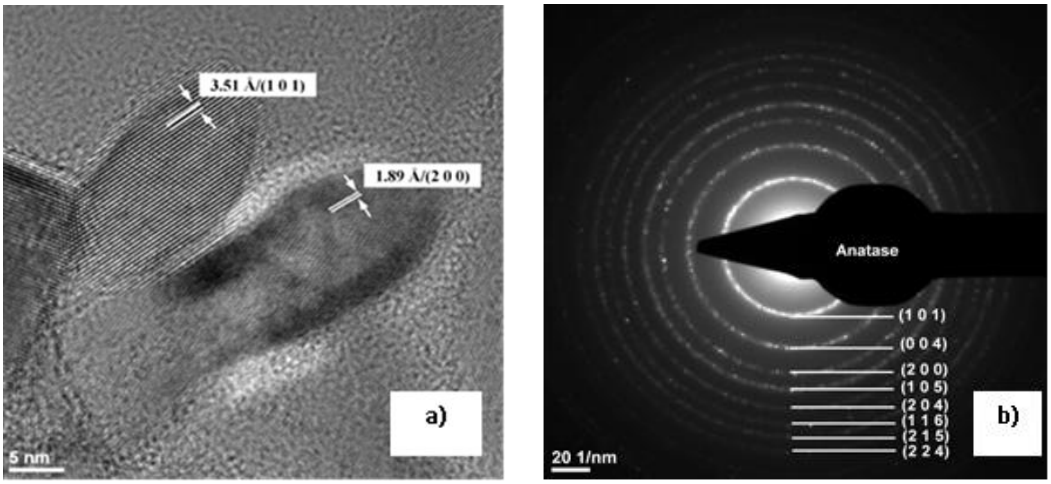

Fig 6. HR-TEM (a) and SAED (b) images of 5 at% Co-doped TiO_2 sample hydrothermally synthesized 120 min. at 250 ^{0}C

3.3 DSC analysis and activation energy of crystallization

The stability of Co-doped anatase nanopowders is a very important parameter for exploiting its specific high surface properties. In order to analyze the phase transformation of Co-doped TiO_2 nanopowders DSC curves of 2.5 and 5 at% Co-doped nanopowders were recorded and compared with un-doped TiO_2 obtained in the same conditions (Fig. 7-10). The results shown are summarized in table 2 where the peak characteristics for samples hydrothermally synthesized at 200^{0}C, 225^{0}C, 250^{0}C, 275 ^{0}C and 120 min are presented.

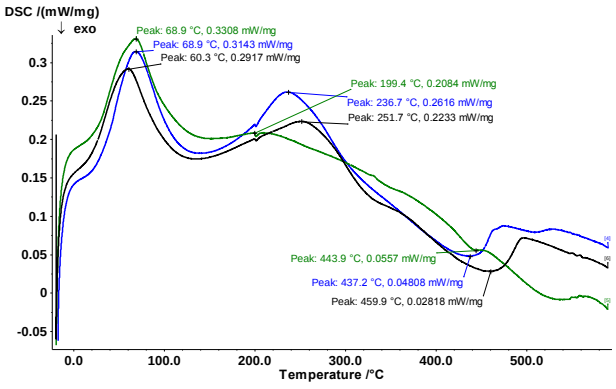

Fig 7. DSC curve of pure and Co-doped TiO_2 synthesized 120 min. at 200°C for a heating rate 10 K min^{-1}

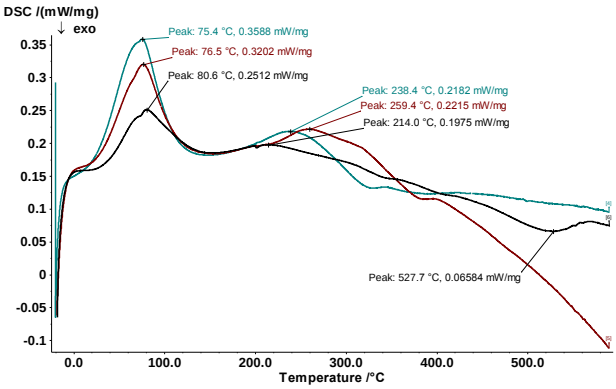

Fig 8. DSC curve of pure and Co-doped TiO_2 synthesized 120 min. at 225°C for a heating rate 10 K min^{-1}

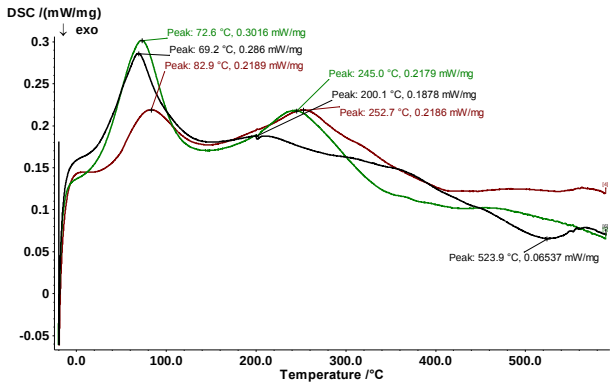

Fig 9. DSC curve of pure and Co-doped TiO_2 synthesized 120 min. at 250°C for a heating rate 10 K min^{-1}

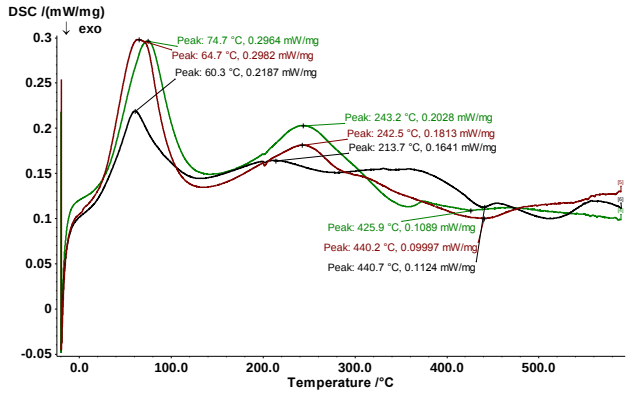

Fig 10. DSC curve of pure and Co-doped TiO_2 synthesized 120 min. at 275°C for a heating rate 10 K min^{-1}

The first endothermic peaks are related to the evaporation of residual solvent adsorbed on the surface. The second endothermic peaks are related to the elimination of -OH groups from the lattice and the third exothermal peak is related to complete crystallization of anatase. All peaks are shifted toward higher temperatures with increasing Co content in the anatase lattice. It may be observed that the enthalpy of crystallization for both pure and Co-doped TiO2 strongly decrease with increasing the hydrothermal synthesis temperature. In other words increasing the synthesis temperature may have a positive impact in controlling the crystallinity of the nanopowders. It may also be observed that crystallization of samples doped with 2.5 and 5 at % Co synthesized at 225^0C and 250^0C is already accomplished during the elimination of OH groups and the third peak is not appearing in the DSC spectra. To explain the reason for this behavior the activation energy and corresponding kinetic model has to be studied.

Table 2. Experimental results on DSC characterization of pure and doped Co-TiO_2 synthesized 120 min. at 200^0C, 225^0C, 250^0C, 275 ^{0}C

	T1 ^{0}C	**ΔH1 J g-1**	**T2 ^{0}C**	**ΔH2 J g-1**	**T3 ^{0}C**	**ΔH3 J g-1**
TiO_2 un-doped at 200^0C	68.9	n.c.	199.4	12.26	443.9	-1225
2.5 Co- dopedTiO_2 at 200^0C	60.3	n.c.	251.7	49.6	459.9	-25.48
5 Co- dopedTiO_2 at 200^0C	68.9	n.c.	236.7	50.67	437.2	-18.43
TiO_2 un-doped at 225^0C	80.6	n.c.	214	5.34	527.7	-8.303
2.5 Co- dopedTiO_2 at 225^0C	76.5	n.c.	259.4	34.68	-	-
5 Co- dopedTiO_2 at 225^0C	75.4	n.c.	238.4	33.97	-	-
TiO_2 un-doped at 250^0C	69.2	n.c.	200.1	5.08	523.9	-8.073
2.5 Co- dopedTiO_2 at 250^0C	82.9	n.c.	252.7	34.12	-	-
5 Co- dopedTiO_2 at 250^0C	72.6	n.c.	245	39.98	-	-
TiO_2 un-doped at 275^0C	60.3	n.c.	213.7	7.003	440.7	- 2.231
2.5 Co- dopedTiO_2 at 275^0C	64.7	n.c.	242.5	7.466	425.9	- 13.27
5 Co- dopedTiO_2 at 275^0C	74.7	n.c.	243.2	21.93	440.7	- 0.59

The iso-conversional methods [23] were further used to calculate the activation energy of hydrothermal crystallization taking into account the experimental values for the third peak.

Considering that the kinetic of crystallization given by

$$v = \frac{d\alpha}{dt} = k(T)\, f(\alpha) \qquad (1)$$

where α is the transformation degree, t is the time and T the absolute temperature, and

$$k(T) = A\exp(-\frac{E}{RT}) \qquad (2)$$

where A is the rate constant pre-exponential factor, E is the activation energy and R is the universal gas constant (8.314472 $JK^{-1}mol^{-1}$) the procedure consisted in calculating the transformation degree best fitting the experimental values for the crystallization peak, considering that crystallization in solid state may be described by the Avrami-Erofeev equation:

$$f(\alpha) = n(1-\alpha)[-\ln(1-\alpha)]^{(1-1/n)} \qquad (3)$$

where n is the reaction order.

The activation energy was calculated using a MATHCAD sub-routine from the slope of the line

$$\ln\left(\frac{\beta\frac{d\alpha}{dT}}{f(\alpha)}\right) = \ln A - \frac{E}{RT} \qquad (4)$$

where the heating rate of the DSC system was $\beta = \frac{dT}{dt} = 10K/\min$.

The calculated values of the activation energy are presented in table 3.

It is worthly to note that the best fitting values for pure TiO2 were obtained for the reaction order n=1, while for the 2.5 and 5 a% Co-doped TiO2 the best fiting values were obtained for n=2/3 with corresponds to the tridimensional movement of the new created phase interface [24]. The modification of the activation energy of crystallization with increasing Co content may be explained by the evolution of lattice deffects concentration. According to [25] cobalt is partially atomically dispersed in the host matrix for the fraction of diluted Co limited to 3 at.%, while for concentrations higher than 0.05, the rest of the Co atoms gather into Co_3O_4 clusters.

Table 3. Calculated activation energies, reaction order and rate constant pre-exponential factors of pure and doped Co-TiO_2 synthesized 120 min. at 200^{0}C, 225^{0}C, 250^{0}C, 275 ^{0}C

Sample	Activation energy	Reaction order	Pre-exponential factor
	kJ mol^{-1}		min^{-1}
TiO_2 un-doped at 200^{0}C	333.414	1	4.914 x 10^{21}
TiO_2 un-doped at 225^{0}C	247.217	1	8.414 x 10^{15}
TiO_2 un-doped at 250^{0}C	493.421	1	6.961 x 10^{31}
TiO_2 un-doped at 275^{0}C	288.578	1	6.936 x 10^{18}
2.5 Co- dopedTiO_2 at 200^{0}C	131.086	2/3	737 x 10^{8}
2.5 Co- dopedTiO_2 at 225^{0}C	180.949	2/3	1.781 x 10^{14}
2.5 Co- dopedTiO_2 at 250^{0}C	121.303	2/3	3.219 x 10^{8}
2.5 Co- dopedTiO_2 at 275^{0}C	131.959	2/3	8.958 x 10^{8}
5 Co- dopedTiO_2 at 200^{0}C	286.694	2/3	2.17 x 10^{21}
5 Co- dopedTiO_2 at 225^{0}C	402.235	2/3	8.842 x 10^{31}
5 Co- dopedTiO_2 at 250^{0}C	346.366	2/3	1.157 x 10^{26}
5 Co- dopedTiO_2 at 275^{0}C	349.055	2/3	7.254 x 10^{26}

3.4 EPR measurements

The analysis of the spectra shows two signals, one near 2000G and the other 3100 G (Fig. 11). These signals correspond to the Co^{2+} ions having the effective $g_{\perp}$ = 3.285 and $g_{//}$ = 2.198 respectively. The sharp line situated at 3400 G could be attributed to the deffect centres implying Ti^{3+} ions. Also it may be observed that by increasing temperatures the Co ions signal is decreasing due to the very high relaxation time. An increase of the line width with the doping concentration appears. This behaviour can be attributed to the spin- spin interactions. By analysing the EPR intensity we can estimate magnetic behaviour of the samples. Our samples present a ferromagnetic behaviour at high temperature.

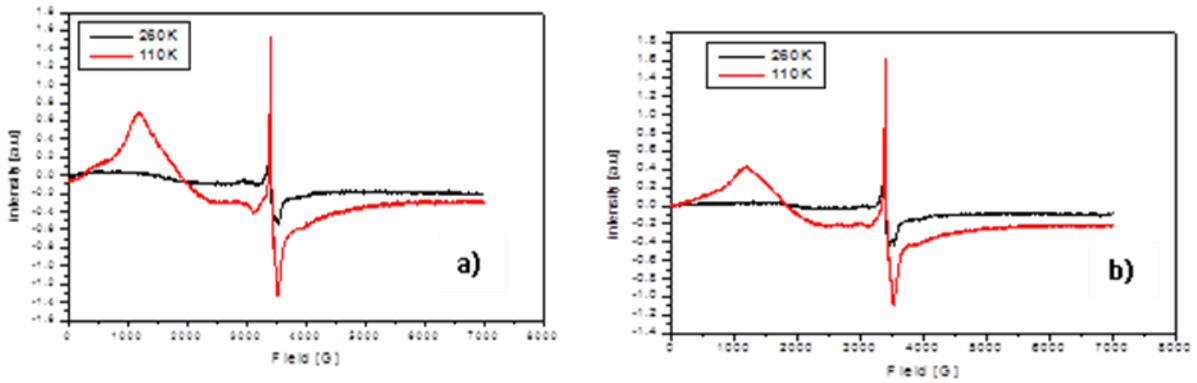

Fig. 11. EPR spectra recorder at two selected temperatures for TiO_2 doped with 2.5%Co (a) and 5% Co respectively (b) synthesized 2 h at 275^{0}C

The ferromagnetic behaviour can be estimated from the integral intensity (I) variation of the EPR spectra which permit to deduce the temperature dependence of the magnetic susceptibility. The temperature dependence of the integral intensity can be described by the equation Eq. (5).

$$I(T) \sim C(x) / (T - \theta(x)) \quad (5)$$

where C is the Curie constant and θ a Curie – Weiss temperature, both depending on x, the dopant concentration. For TiO_2 powders doped with 2.5% Co ferromagnetic behaviour was obtained in 110-240 K temperature range.

As far as TiO_2 powders doped with 2.5% Co samples are concerned, EPR investigations show two ferromagnetic domains as function of temperature. In the low temperature range 110-160 K, the evaluated θ value is 110 K, while in the high temperature range 170-230 K a value of 165 K is obtained. It could mean that at higher temperatures the exchange interaction between Co ions increases leading to an increase of the Curie-Weiss temperature.

4. Conclusions

Co-doped TiO_2 nanopowders with 100% anatase structure and rod-like morphology were prepared using hydrothermal synthesis. The kinetics of the hydrothermal crystallization is controlled by selecting temperature, time and concentration of mineralizing agent.

For pure TiO_2 the best fitting reaction order is n=1 while for 2.5 and 5 at% Co-doped TiO_2 the reaction order is n=2/3. The mean activation energy of crystallization calculated from DSC measurements are respectively 340.6 kJ mol^{-1} for pure TiO_2, 141.3 kJ mol^{-1} for 2.5 at% Co doped TiO_2 and 346.1 kJ mol^{-1} for 5 at% Co doped TiO_2. The modification of the activation energy of crystallization with increasing Co content may be explained by the evolution of lattice deffects concentration. The evolution of the activation energy with Co concentration may be explained by the Co partially atomically dispersed in the host matrix for the fraction of diluted Co limited to 3 at.%, while for concentrations higher than 0.05, the rest of the Co atoms gather into Co_3O_4 clusters. The EPR measurments on Co-doped TiO_2 powders show also the modification of the ferromagnetic behaviour with incresing doping content from 2.5 % Co to 5 % Co. The results are promising for the use of these materials in spintronic applications.

Acknowledgements

We gratefully acknowledge the financial support in the frame of the research contract PCCE-ID 106/2008 supported by Romanian Unity for the Financing of High Education, Research, Development and Innovation (UEFISCDI).

References

[1] A.K. Pradhan, D. Hunter, B.D. Hunter, J.B. Dadson, K. Zhang, R.R. Rakhimov, J. Appl. Phys. **99**, 08M108-1-3 (2006).
[2] M. Bibes, M. Bowen, A. Barthelemy, A. Anane, K. Bouzehouane, C. Carratero E. Jacquet, J.-P. Contour, Appl. Phys. Lett. **82**, 3269 (2003).
[3] Y.G. Joh, H.D. Kim, B.Y. Kim, S.I. Woo, S.H. Moon, J.H. Cho, E.C. Kim and D.H. Kim., J. Appl.Korean Phys. Soc. **44i** , 360 (2004).
[4] N.N. Hai, N.T. Khoi, P.V. Vinh, J.Phys:Conf. Series **187**, 1 (2009) -8
[5] L.C.J. Perreira, M.R. Nunes, O.C. Monteiro, A.J. Silvestre, Appl. Phys. Lett. **93,** 222502-1 (2008).
[6] X. Chen, S.S. Mao, Chem. Rev. **107,** 2891 (2007).
[7] M. Abrudeanu, R.R. Piticescu, R.M. Piticescu, Wet chemical synthesis of ultradisperse ceramic powders, Editura Tehnica Bucharest (1999), p. 68-80
[8] D.L. Morgan, H.W. Liu, R.L. Frost, E.R. Waclawik, J. Phys. Chem. C **114,** 101 (2010) .
[9] R. M. Nunes, O. C. Monteiro, A. L. Castro D.A.Vasconcelos, A.J. Silvestre, Eur J.Inorg.Chem. (2008) 961.
[10] Y. Hwu, Y.D. Yao, N.F. Cheng, C.Y. Tung, H.M. Lin, Nanostruct. Mater. **9**, 355 (1997)
[11] H. Zhang, J.F.L. Banfield, Mater. Chem. **8,** 2073 (1998).
[12] A.A. Gribb, J.F. Banfield, Am. Mineral. **82,** 717 (1997).
[13] M.R. Ranade, A. Navrotsky, H.Z. Zhang, J.F. Banfield, S.H. Elder, A. Zaban, P.H. Borse, S.K. Kulkarni, G.S. Doran, H.J. Whitfield, Proc. Natl. Acad. Sci. 99 (2002), 6476.
[14] W. Li, C. Ni, H. Lin, C.P. Huang, S.I. Shah, J. Appl. Phys. **96**, 6663 (2004).
[15] B.D. Stojanovic, Z.V Marinkovic, G.O. Brankovic, E. Fidancevska, JTAC **60**, 595 (2000).
[16] H. Mehranpour, M. Askari, M. S. Ghamsari, H. Farzalibeik, J. Nanomaterials, ID 626978 (2010).
[17] V. Balek, N. Todorova, C. Trapalis, V. Stengl, E. Vecernika, J. Subrt, Z. Malek, G. Kordas, JTAC **80,** 503 (2005).
[18] H.I. Hsiang; C.L Shih, J.Mater. Chem. Phys. 95, 275 (2006).
[19] Z. Hengzhong, J. F. Banfield, Chem. Mater. **14**, 4145 (2002).
[20] R.Campostrini, M. Ischia, L. Palmisano, JTAC **71,** 997 (2003).
[21] R.Campostrini, M. Ischia, L. Palmisano, JTAC **71** 1011 (2003)
[22] R.R. Piticescu, S. Valsan, O. Raita, Romanian Patent Request A/01285 nr. ref. 2122/30.11.2011
[23] Michael E. Brown, Introduction to Thermal Analysis, second ed., Kluwer Academic Publishers, Dordecht/Boston/London, 2001, pp. 181-210
[24] L. A. Perez Maqueda, J. M. Criado, F. J. Gotor, J. Malek, J. Phys. Chem., **106**, 2862 (2002)
[25] M. N. Grecu, D. Macovei, D. Ghica, C. Logofatu, S. Valsan N.G. Apostol, G.A. Lungu, R.F. Negrea, R.R. Piticescu, Appl. Phys. Lett. **102**, 161909 (2013); doi: 10.1063/1.4802819

*Corresponding author: atudor@imnr.ro